BIOCHEMISTRY
including biophysical chemistry & molecular biology

Article

pubs.acs.org/biochemistry

Efficiencies of Activation of Transducin by Cone and Rod Visual Pigments

Yasushi Imamoto, Ichirota Seki, Takahiro Yamashita, and Yoshinori Shichida*

Department of Biophysics, Graduate School of Science, Kyoto University, Kyoto 606-8502, Japan

Supporting Information

ABSTRACT: How the light-induced transducin (Gt) activation process differs biochemically between cone visual pigments and rod visual pigment (rhodopsin) has remained unclear, because the Gt-activating state (Meta-II) of cone visual pigment decays too fast to precisely measure the activation efficiency by conventional biochemical methods such as the GTPγS binding assay. Here we measured the activation efficiencies of chicken green-sensitive cone visual pigment (cG) and bovine rhodopsin (bRh) in real time by monitoring the intrinsic fluorescence of tryptophan residues in the pigments and Gt. Michaelis–Menten analysis of Gt activation showed that the initial velocity for cG was approximately half that for bRh, while their Michaelis constants were comparable. Gt activation by cG was immediately slowed because of the fast hydrolysis of the retinal Schiff base in Meta-II, but this hydrolysis was suppressed by forming the complex with Gt. Using mutants of cG and bRh for positions 122 and 189, which exhibit altered rates of chromophore hydrolysis in Meta-II, we found that the initial velocity of Gt activation is negatively correlated with the rate of chromophore hydrolysis. These results suggest that the amino acid residues at positions 122 and 189 account for not only the resistance to the chromophore hydrolysis in Meta-II but also the conformation of Meta-II for efficient Gt activation. The substantially longer lifetime of the Gt activating state of Rh would be necessary to suppress the spontaneous quenching by the stochastic decay of the Gt-activating state when a rod responds to a single photon.

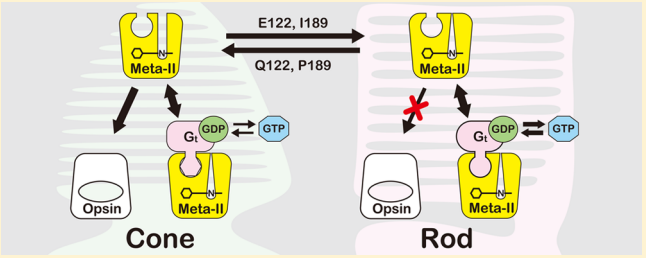

The visual transduction process in photoreceptor cells begins with the absorption of photons by visual pigments, which are members of the family of G protein-coupled receptors. There are several types of cone visual pigments but only one type of rod visual pigment (rhodopsin) in the retinas of vertebrates. These pigments are expressed in cone and rod photoreceptor cells responsible for photopic and scotopic vision, respectively. Phylogenetic analysis of cone visual pigments and rhodopsin has indicated that an ancestral visual pigment diverged first into four groups of cone visual pigments, and the rhodopsin group diverged from one of the groups of cone visual pigments.[1] Therefore, it is of interest to examine what kinds of molecular properties of rhodopsin have been acquired to meet the requirements of scotopic vision in the course of molecular evolution. One of the most prominent differences in the cell responses between rods and cones lies in their photosensitivity, which may possibly be explained by differences in the molecular properties between cone visual pigments and rhodopsin.

Extensive comparative studies of the photochemical properties of cone visual pigments and rhodopsin have been reported previously.[2−7] They showed that although the photosensitivities of the cone visual pigment and rhodopsin are quite similar, the intermediate state of the cone visual pigment (Meta-II) that activates G protein transducin (Gt) decays significantly faster than that of rhodopsin, mainly because of the residues at positions 122 and 189.[8,9]

To assess the difference in Gt activation between the cone visual pigment and rhodopsin, kinetic analyses of the interaction between Meta-II and Gt are essential. However, the decay of Meta-II of the cone visual pigment is too fast to monitor the interaction by conventional biochemical techniques such as the radiolabeled GTPγS binding assay. In general, optical measurements are advantageous for time-resolved analysis. In fact, time-resolved tryptophan fluorescence measurements have been applied to monitor the decay of metarhodopsin II and its Gt activation process.[10−15] Thus, it is desirable to apply optical measurements to monitor the process of Gt activation by cone visual pigments.

Phylogenetic analyses have demonstrated that the rhodopsin group evolved from the M2 group of cone pigments. Because the phylogenetic groups of visual pigments extend over various classes of animals, comparative studies of the cone visual pigment of the M2 group and rhodopsin are highly suitable for highlighting the difference between rod and cone visual transduction systems. In this study, we characterized the interaction between Gt and chicken green-sensitive cone pigment (cG) by a fluorescence assay based on Michaelis–Menten kinetics.

Received: November 28, 2012
Revised: April 9, 2013
Published: April 9, 2013

MATERIALS AND METHODS

Sample Preparation. Genes of cG and bRh were expressed in HEK293S cells as reported previously.[16,17] Pigments were reconstituted by adding 11-*cis*-retinal, solubilized using *n*-dodecyl *β*-D-maltoside (DDM), and adsorbed to a 1D4 immunoaffinity column.[17] The column was washed extensively to remove impurities and excess retinal before elution. It is possible that the expression and purification procedure could influence the properties of the recombinant pigment, but the UV−visible absorption spectrum suggested that the chromophore was accommodated in a manner similar to that of native pigments. Mutants of bRh and cG (bRh-E122Q/I189P and cG-Q122E/P189I) were prepared similarly.[8,18]

The bovine rod Gt heterotrimer was extracted from irradiated bovine rod outer segment membranes by adding GTP and purified by DEAE Toyopearl 650S (Tosoh, Tokyo, Japan) column chromatography as reported previously.[19] The activity of Gt in the preparation was estimated by fluorescence titration with GTP*γ*S and AlFx, which showed that >85% of Gt in the preparation was active. The bovine rod Gt heterotrimer was used in all experiments presented here.

HAP, an 11-mer peptide analogous to the C-terminus of the Gt *α*-subunit (NH_2-VLEDLKSCGLF-COOH), which shows high affinity for photoactivated rhodopsin,[20] was synthesized by Kurabo (Osaka, Japan).

All measurements were taken using the same reaction buffer [0.01% DDM, 40 mM HEPES, 30 mM NaCl, 60 mM KCl, 2 mM $MgCl_2$, and 1 mM dithiothreitol (pH 7.5)].

Spectroscopy. Transient UV−visible absorption spectra after flash irradiation were recorded using a high-speed multichannel spectrophotometer (C10000 system, Hamamatsu Photonics, Shizuoka, Japan).[21] The temperature of the sample was kept at 20 °C by a temperature-controlled cuvette holder utilizing a Peltier device (qpod, Ocean Optics, Dunedin, FL). A flash light for irradiation of the pigment was generated by a short-arc xenon flash lamp (SA-200F, Nissin Electronic, Tokyo, Japan; pulse duration of ∼170 *μ*s) and filtered by an optical filter (Y52, Asahi Techno Glass, Chiba, Japan).

Slow fluorescence changes (∼5 min) were monitored using a Shimadzu (Kyoto, Japan) RF-5300PC spectrofluorophotometer. Excitation and emission wavelengths were set at 300 and 340 nm, respectively. The pigment was irradiated with yellow light that was generated by a 1 kW tungsten−halogen lamp (HIRUX-HR, Rikagaku, Tokyo, Japan) and filtered with a yellow glass filter (Y50 or Y52, Asahi Techno Glass). The temperature of the sample was kept at 20 °C.

Fast fluorescence changes (<20 s) were monitored using a laboratory-constructed photon counting system. Briefly, an excitation beam at 300 nm was generated by a xenon lamp (SO-X150, JASCO, Tokyo, Japan) and a monochromator (CT-10, JASCO). Fluorescence was detected by a photon counting head (H7360-01, Hamamatsu Photonics) connected to a controller unit (C8855, Hamamatsu Photonics). Fluorescence greater than 310 nm was collected using a band-pass filter (U-360) in front of the photon counting head. The counting duration was 100 ms. The pigments were irradiated with a flash light generated by a combination of a short-arc xenon flash lamp (SA-200F, Nissin Electronic) and an optical filter (O54, Y52, or Y50, Asahi Techno Glass). The temperature of the sample was kept at 20 °C. The validity of the data obtained using this laboratory-constructed fluorophotometer was confirmed by their consistency with those obtained using a conventional fluorophotometer (Shimadzu RF-5300PC).

Because the absorption spectra of bRh, cG, and the mutants were different from each other, the fraction of bleached pigment produced by a flash irradiation (p_{bleach}) varied. p_{bleach} was estimated by UV−visible absorption spectroscopy using a Shimadzu UV2400PC spectrophotometer.

Data Analyses. The time courses of absorption changes and fluorescence changes were analyzed according to the schemes shown below. The curve fitting and singular-value decomposition (SVD) analysis were conducted using Igor Pro version 5.0 (WaveMetrics, Lake Oswego, OR).

RESULTS

Photobleaching Process of DDM-Solubilized cG. We first investigated the photobleaching process of DDM-solubilized cG at 20 °C by means of UV−visible absorption spectroscopy. cG in 0.01% DDM buffer (curve 1 in Figure 1a) was irradiated with a yellow flash, and the spectral changes were recorded from 2 ms to 100 s (curves 2−5 in Figure 1a). Figure 1b shows the decay-associated difference spectra (B spectra)

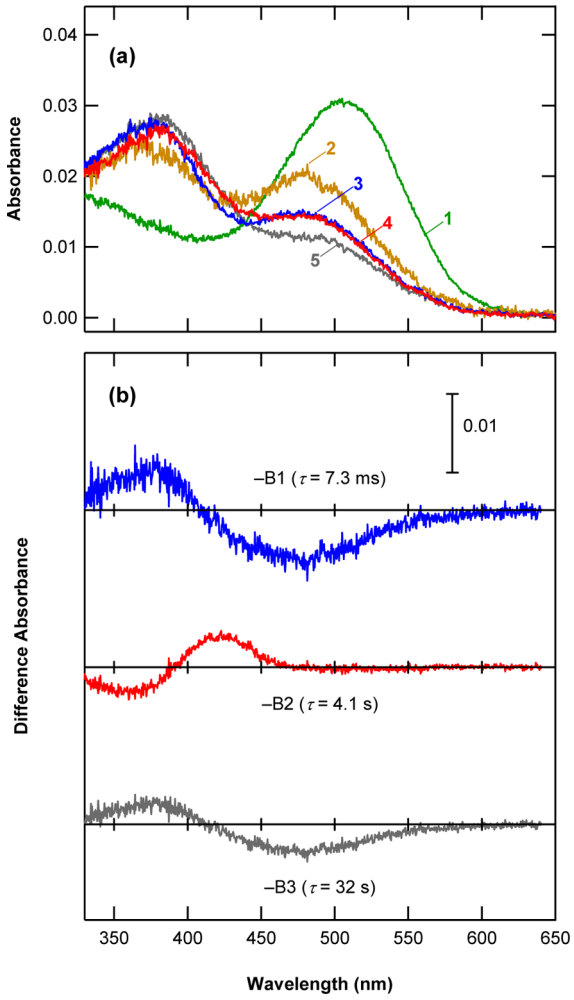

Figure 1. Photobleaching process of cG. (a) cG in the dark (curve 1) was irradiated with a yellow flash at 20 °C, and the transient absorption spectra were measured. Typical spectra measured 2 ms, 1 s, 8 s, and 100 s after flash irradiation are shown (curves 2−5, respectively). (b) Decay-associated difference spectra for the spectral changes in panel a. The time constants are shown.

dx.doi.org/10.1021/bi3015967 | *Biochemistry* 2013, 52, 3010−3018

calculated by SVD analysis of the spectral changes followed by global fitting of V spectra[22] (Figure S1 of the Supporting Information). The photobleaching process of cG on the time scale of 10^{-3} to 10^{2} s was represented by three reaction components (B1−B3 spectra) with time constants ($1/k$) of 7.3 ms, 4.1 s, and 32 s, respectively. The B1−B3 spectra are consistent with the difference spectra between curves 2 and 3, curves 3 and 4, and curves 4 and 5, respectively. The B3 spectrum shows the decay of 480 nm species into 380 nm species, while the B2 spectrum shows a small red shift of 375 nm species (curves 3 and 4). Therefore, B2 and B3 spectra are likely to show the conversion from Meta-II to all-*trans*-retinal with opsin and that from Meta-III to all-*trans*-retinal with opsin, respectively. Thus, the B1 spectrum should represent the conversion from Meta-I to a mixture of Meta-II and Meta-III.

We previously reported that the photobleaching of cG solubilized by CHAPS-PC was represented only by two reaction components: one being the conversion from Meta-I to a mixture of Meta-I, Meta-II, and Meta-III and the other that from this mixture to all-*trans*-retinal with opsin.[23] However, DDM-solubilized cG exhibited an additional reaction component represented by the B2 spectrum, which is similar in shape to the difference spectrum between Meta-II and all-*trans*-retinal. Therefore, in DDM-solubilized cG, decomposition of Meta-II into all-*trans*-retinal with opsin is much faster than the decomposition of Meta-III and back reaction from Meta-III to Meta-I and/or Meta-II.

The absorbance decrease at 480 nm, showing the decay of Meta-I, was not observed in the B2 spectrum. Thus, it is likely that the equilibrium between Meta-I and Meta-II of cG in DDM buffer is biased toward Meta-II as that between metarhodopsin I and metarhodopsin II.[24] The amount of Meta-III was estimated to be 26% of the total photoactivated cG from the absorbance decrease at 480 nm in the B3 spectrum using the ratio of molar extinction coefficients of Meta-III and cG.[18]

Increase in the Fluorescence of cG upon Irradiation. We next monitored the change in the Trp fluorescence of cG after flash irradiation using a laboratory-constructed fluorophotometry system (Figure 2a). The Trp residue is an excellent intrinsic fluorescence probe for monitoring the activation of Gt and dissociation of all-*trans*-retinal from bleached visual pigments.[10−15] Unlike the fluorescence of extrinsic probes such as Alexa Fluor,[25] the fluorescence of Trp cannot be generated by red light, which hardly bleaches rhodopsin, but unmodified proteins can be used. Here we used 300 nm excitation light to generate Trp fluorescence, which may cause the bleaching of preactivated visual pigments and/or artifactual photoreaction of Meta-II. To detect Trp fluorescence generated by a faint excitation light, we constructed a photon counting system that allowed us to measure the fluorescence without a significant bleach of visual pigment (1%/min). Using this system, the intrinsic fluorescence of cG was characterized.

It has been reported that the intrinsic fluorescence of the photoactivated visual pigment is increased upon the release of all-*trans*-retinal.[13−15] The fluorescence intensity of photoactivated cG increased rapidly with a time constant of 2.9 s (Figure 2a). Because this time constant was consistent with the time constant for the B2 spectrum (4.1 s) (Figure 1b), it is likely that this fluorescence increase represents the decay of Meta-II to opsin. To confirm that, the fluorescence increase was examined in the presence of bovine rod Gt or HAP,[20] which form a stable complex with metarhodopsin II (extra-

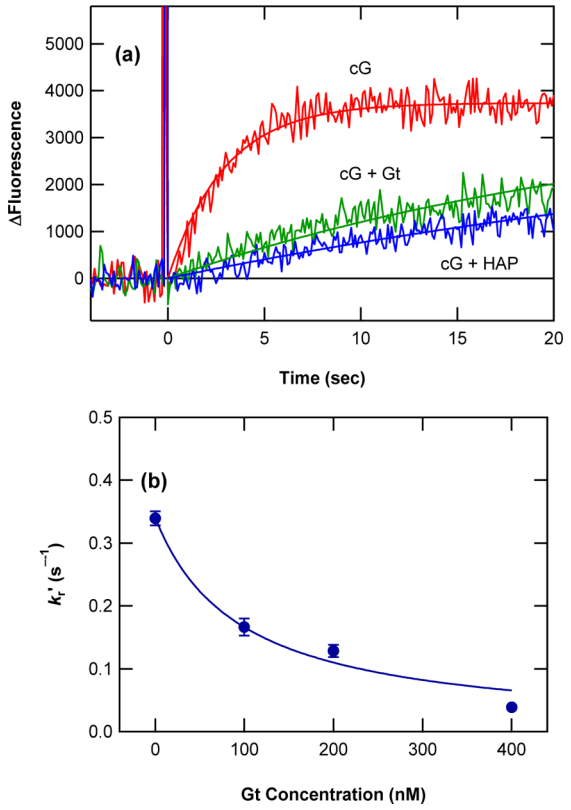

Figure 2. Intrinsic fluorescence increase of cG. (a) Intrinsic fluorescence of cG (12 nM; p_{bleach} = 0.76) generated by excitation at 300 nm. cG was irradiated with a yellow flash at time zero, and the fluorescence change was monitored at 20 °C (top trace). The fluorescence increase was suppressed in the presence of 400 nM Gt (middle trace) or 100 nM HAP (bottom trace). (b) Apparent rate constant (k_r') of fluorescence increase plotted vs Gt concentration. It was fit by eq 4, giving a K_d of 95 ± 21 nM.

metarhodopsin II) in the absence of GTP.[26] As expected, Gt and HAP suppressed the increase in the fluorescence of cG, showing the formation of a stable complex of Meta-II with Gt or HAP. Because HAP has no Trp residue that would generate fluorescence and there is no activation of Gt in the absence of GTP, this fluorescence increase is solely due to formation of cG opsin.

To characterize the Meta-II·Gt complex of cG, the dependence of the rate of increase in the fluorescence on the Gt concentration was examined (Figure 2b). The rate was analyzed according to Scheme 1, where Meta-II and Gt form

Scheme 1. Formation of Opsin from Meta-II and the Meta-II·Gt Complex

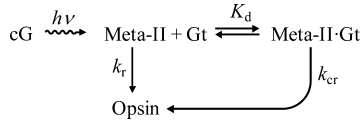

the Meta-II·Gt complex with a dissociation constant K_d, and opsin is formed from both Meta-II and the Meta-II·Gt complex with rate constants of k_r and k_{cr}, respectively. The presence of Meta-I and Meta-III was not taken into consideration in the kinetic analysis below because (1) SVD analyses showed that the thermal equilibrium between Meta-I and Meta-II is significantly biased toward Meta-II in DDM buffer (B2 in

dx.doi.org/10.1021/bi3015967 | *Biochemistry* 2013, 52, 3010−3018

Figure 1b), (2) Meta-III was likely to be produced from Meta-I (B1 in Figure 1b) within the time resolution of the fluorescence measurements (time constant of 7.3 ms, time resolution of 100 ms), and (3) Meta-III decays significantly more slowly (time constant of 32 s) than Meta-II (4.1 s) and the amount was small (26%). These findings indicate that the fluorescence increase over the first few seconds after irradiation represents the formation of opsin from the mixture of Meta-II and the Meta-II·Gt complex.

The velocity of opsin formation from Meta-II and/or the Meta-II·Gt complex in Scheme 1 is expressed as follows:

$$\frac{d[\text{opsin}]}{dt} = k_r[\text{Meta-II}] + k_{cr}[\text{Meta-II·Gt}] \quad (1)$$

Under the approximation of [Gt] ≫ [Meta-II·Gt], the velocity of opsin formation is expressed as follows using the initial concentration of total Meta-II ($[\text{Meta-II}]_{t=0}^{\text{total}}$ = [Meta-II] + [Meta-II·Gt] + [opsin]) and the dissociation constant of the Meta-II·Gt complex [K_d = ([Meta-II][Gt])/[Meta-II·Gt]]:

$$\frac{d[\text{opsin}]}{dt} = \frac{k_r K_d + k_{cr}[\text{Gt}]}{K_d + [\text{Gt}]}([\text{Meta-II}]_{t=0}^{\text{total}} - [\text{opsin}]) \quad (2)$$

Therefore, the concentration of opsin at time t is expressed as follows:

$$[\text{opsin}] = [\text{Meta-II}]_{t=0}^{\text{total}}[1 - \exp(-k_r' t)] \quad (3)$$

where

$$k_r' = \frac{k_r K_d + k_{cr}[\text{Gt}]}{K_d + [\text{Gt}]} \quad (4)$$

Fluorescence increases of cG in the presence of various concentrations of Gt but no GTP were measured and fit to eq 3 to obtain k_r'. k_r' was then plotted against Gt concentration and fit with eq 4 with the following constraints: $k_r \geq 0$, and $k_{cr} \geq 0$ (Figure 2b). The fitting gave a K_d of 95 nM, a k_r of 0.34 s^{-1}, and a k_{cr} of ~0 s^{-1}. The fact that k_{cr} was close to 0 indicates that the Gt binding almost completely inhibits the hydrolysis of the retinal Schiff base.

Comparison of Gt Activation Efficiency between cG and bRh. Metarhodopsin II catalyzes the GDP−GTP exchange reaction on the Gt α-subunit, resulting in the dissociation of the activated α-subunit from the $\beta\gamma$-subunits, which can be observed by the increase in the intrinsic fluorescence of Trp207 in the α-subunit.[11] We first examined whether a similar fluorescence assay is useful for monitoring activation of Gt by cG.

bRh or cG was mixed with bovine rod Gt and GTPγS, and the fluorescence was measured with the 300 nm excitation light using a conventional fluorophotometer (Figure 3). In these experiments, a nonhydrolyzable GTP analogue, GTPγS, was used to avoid the inactivation of Gt by the endogenous hydrolysis of GTP. After the measurement of the baseline, the pigment was completely bleached by irradiation with yellow light for 6 s, and the fluorescence was further measured. As a control, the fluorescence of bRh or cG in the absence of Gt and GTPγS was measured.

For the rhodopsin sample, the fluorescence of Gt was increased by irradiation, showing the activation of Gt by photoactivated rhodopsin, while a small increase in the fluorescence of rhodopsin was also observed without Gt and GTPγS. Therefore, the net increase in fluorescence caused by

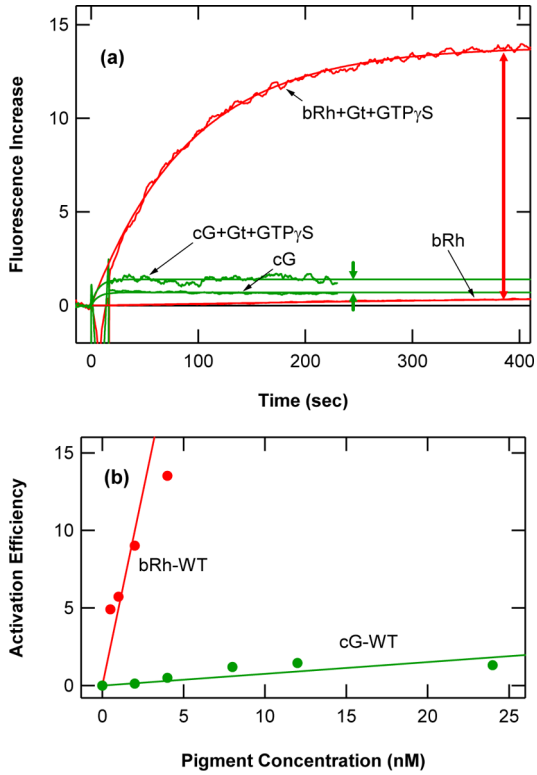

Figure 3. Activation of Gt by bRh and cG. (a) bRh or cG (either at 4 nM) was mixed with 400 nM Gt and 200 μM GTPγS. The mixture was irradiated at time zero for 6 s, and the fluorescence increase was monitored at 20 °C. The fluorescence increase due to opsin formation was separately recorded in the absence of Gt and GTPγS. (b) Net fluorescence increase of Gt activation (arrows in panel a) plotted vs pigment concentration when concentrations of Gt and GTPγS were constant (400 nM and 200 μM, respectively). While the plot for bRh was not linear because of the depletion of Gt, it was fit with a straight line for the sake of simplification.

Gt activation is shown by the difference between the fluorescence increase in the presence and absence of Gt and GTPγS (arrows in Figure 3a).

The same measurements were taken using cG. The fluorescence was increased even in the absence of Gt and GTPγS as a result of the rapid release of all-*trans*-retinal, as shown in Figure 2. However, in the presence of Gt and GTPγS, a further fluorescence increase was observed. This difference represents the fluorescence increase of Gt activated by cG (arrows in Figure 3a), indicating that the activation of Gt by cG can be quantitatively evaluated by fluorescence measurements, like Gt activation by rhodopsin. It should be noted that no further fluorescence increase was observed for cG after irradiation. Because of the rapid hydrolysis of the Schiff base (Figure 2), Meta-II of cG would be almost fully decayed after irradiation for 6 s.

The efficiency of activation by bRh and cG was estimated at various pigment concentrations (Figure 3b). From the slopes of the regression lines, the efficiency of Gt activation by bRh was estimated to be 70 times higher than that by cG.

Kinetic Characterization of Gt Activation by the Cone Visual Pigment. To assess the cause of the low Gt activation efficiency of cG, the kinetics of activation were analyzed in detail using a laboratory-constructed fluorophotometry system. Fluorescence changes of a bRh/Gt/GTPγS mixture (Figure 4a) or a cG/Gt/GTPγS mixture (Figure 4b) after irradiation by a

dx.doi.org/10.1021/bi3015967 | *Biochemistry* 2013, 52, 3010−3018

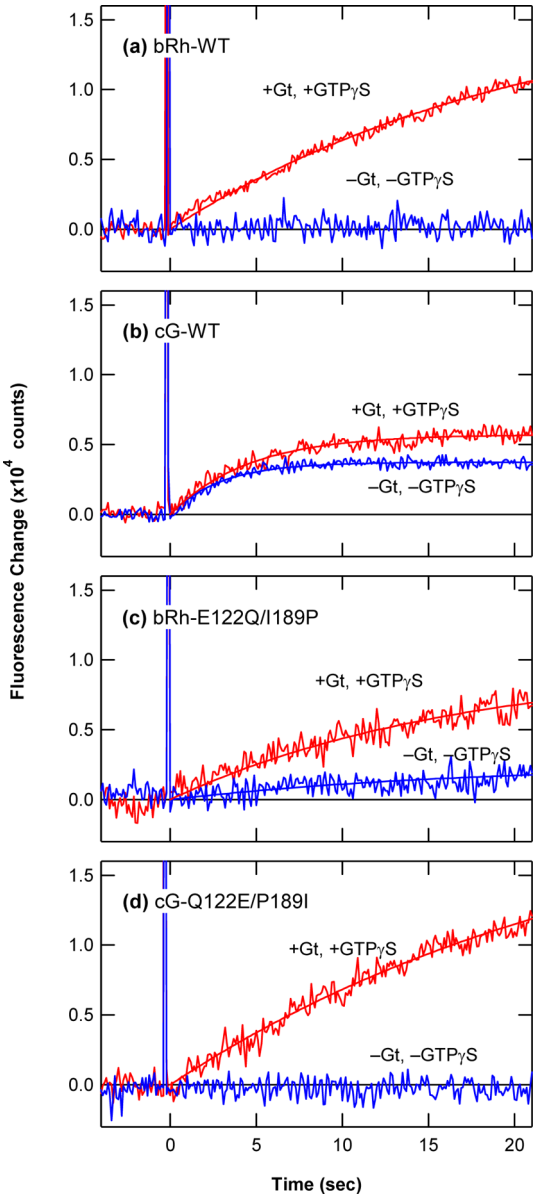

Figure 4. Fluorescence increase resulting from Gt activation after irradiation of the pigments. Pigment (12 nM) was mixed with 400 nM Gt and 200 μM GTPγS. The mixture was irradiated by a yellow flash at time zero, and the fluorescence change was monitored at 20 °C (top traces). The fluorescence increase resulting from opsin formation was measured in the absence of Gt and GTPγS (bottom traces). (a) For bRh-WT, p_{bleach} = 0.75. (b) For cG-WT, p_{bleach} = 0.76. (c) For bRh-E122Q/I189P, p_{bleach} = 0.52. (d) For cG-Q122E/P189I, p_{bleach} = 0.80.

yellow flash were monitored using the photon counting system. Before irradiation, the fluorescence intensity was constant for both samples, indicating that the exposure of the sample to the excitation beam bleached a negligible amount of pigment in this experimental setup.

The fluorescence intensity of the bRh/Gt/GTPγS mixture was increased by flash irradiation (Figure 4a, top trace), whereas that of bRh alone showing opsin formation was negligible (bottom trace). Thus, the initial velocity of the fluorescence increase due to Gt activation $[V_0^{F(Gt\rightarrow Gt^*)}]$ by bRh was obtained from the slope of the line fit to the fluorescence increase of the bRh/Gt/GTPγS mixture (top trace). In contrast to the that of the bRh sample, the fluorescence increase of the cG/Gt/GTPγS mixture immediately reached a plateau (top trace in Figure 4b). It is likely that Meta-II readily decays, resulting in the deceleration of Gt activation. In fact, a fluorescence increase showing opsin formation was observed for Gt alone on this time scale (bottom trace), while it was significantly suppressed by Gt in the absence of GTPγS (Figure 2a). Therefore, the fluorescence increase in the cG/Gt/GTPγS mixture can be attributed to not only Gt activation but also opsin formation. However, the fluorescence increase of Gt activation is not equal to the simple difference between the fluorescence increase in the presence and absence of Gt and GTPγS, because the decay of Meta-II in the presence of Gt should be slower than that in the absence of Gt because of the transient formation of the Meta-II·Gt complex, in which Meta-II is stable (Figure 2). Therefore, the fluorescence increase of the cG sample was analyzed on the basis of the Michaelis–Menten kinetics as follows (Scheme 2).

Scheme 2. Michaelis–Menten Model for Gt Activation by Photoactivated Pigments

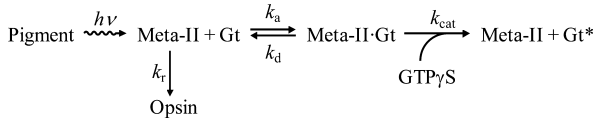

In Scheme 2, Meta-II and Gt first form a Meta-II·Gt complex and a GDP–GTPγS exchange reaction on the Gt α-subunit is catalyzed, resulting in an increase in the fluorescence of Gt. The initial velocity of Gt activation is expressed as follows:

$$V_0 = \frac{k_{cat}[\text{Meta-II}]^{total}[\text{Gt}]}{K_M + [\text{Gt}]} \quad (5)$$

where $K_M = (k_d + k_{cat})/k_a$. Here Meta-II of cG exponentially decays during Gt activation (Figure 2a).

$$[\text{Meta-II}]^{total} = [\text{Meta-II}] + [\text{Meta-II·Gt}] = [\text{Meta-II}]^{total}_{t=0} \exp(-k_r' t) \quad (6)$$

where apparent rate constant k_r' depends on the ratio of Meta-II to the Meta-II·Gt complex (Figure 2b). Because the fluorescence increase of the cG/Gt/GTPγS mixture reached a plateau before the depletion of Gt, the concentration of Gt was assumed to be constant. These equations become

$$V_0 = \frac{d[\text{Gt}^*]}{dt} = \frac{k_{cat}[\text{Meta-II}]^{total}_{t=0}[\text{Gt}]}{K_M + [\text{Gt}]} \times \exp(-k_r' t) \quad (7)$$

Therefore

$$[\text{Gt}^*] = \frac{k_{cat}[\text{Meta-II}]^{total}_{t=0}[\text{Gt}]}{k_r'(K_M + [\text{Gt}])} \times [1 - \exp(-k_r' t)] \quad (8)$$

Equation 8 implies that the increase in the concentration of Gt* is expressed by an exponential function with the apparent rate constant of Meta-II decay (k_r'). The total fluorescence increase at time t (ΔF_t^{total}) is the sum of fluorescence increases for opsin formation ($\Delta F_t^{MII\rightarrow Ops}$) and Gt activation ($\Delta F_t^{Gt\rightarrow Gt^*}$). It is expressed as follows:

$$\Delta F_t^{total} = \Delta F_t^{MII\rightarrow Ops} + \Delta F_t^{Gt\rightarrow Gt^*} = (\Delta F_\infty^{MII\rightarrow Ops} + \Delta F_\infty^{Gt\rightarrow Gt^*})[1 - \exp(-k_r' t)] \quad (9)$$

dx.doi.org/10.1021/bi3015967 | Biochemistry 2013, 52, 3010–3018

The velocity of total fluorescence increase at time t is

$$V_t^{F(\text{total})} = V_t^{F(\text{Gt}\rightarrow\text{Gt}^*)} + V_t^{F(\text{MII}\rightarrow\text{Ops})} = k_r' (\Delta F_\infty^{\text{MII}\rightarrow\text{Ops}} + \Delta F_\infty^{\text{Gt}\rightarrow\text{Gt}^*}) \times \exp(-k_r' t) \quad (10)$$

where $V_t^{F(\text{MII}\rightarrow\text{Ops})}$ and $V_t^{F(\text{Gt}\rightarrow\text{Gt}^*)}$ are the velocities of fluorescence increases for opsin formation and Gt activation, respectively. Therefore, the initial velocity of Gt activation is calculated as follows:

$$V_0^{F(\text{Gt}\rightarrow\text{Gt}^*)} = k_r' (\Delta F_\infty^{\text{total}} - \Delta F_\infty^{\text{MII}\rightarrow\text{Ops}}) \quad (11)$$

When the fluorescence increase for the mixture of 12 nM cG (p_{bleach} = 0.76), 400 nM Gt, and 200 μM GTPγS (Figure 4b) was fit with eq 9, $\Delta F_\infty^{\text{total}}$ and k_r' were estimated to be 5730 counts and 0.22 s^{-1}, respectively. Fitting of the fluorescence increase for the sample containing cG alone gave 3740 counts for $\Delta F_\infty^{\text{MII}\rightarrow\text{Ops}}$. Thus, $V_0^{F(\text{Gt}\rightarrow\text{Gt}^*)}$ was calculated to be 440 counts/s.

$V_0^{F(\text{Gt}\rightarrow\text{Gt}^*)}$ for cG at various Gt concentrations was similarly estimated, whereas that of bRh was simply estimated from the slope for the bRh/Gt/GTPγS mixture. The initial velocity of Gt activation per photoactivated pigment (V_0) was calculated and plotted versus the concentration of Gt, which was fit with the Michaelis–Menten equation as follows (Figure 5):

$$V_0 = V_{\max} \frac{[\text{Gt}]}{K_M + [\text{Gt}]} \quad (12)$$

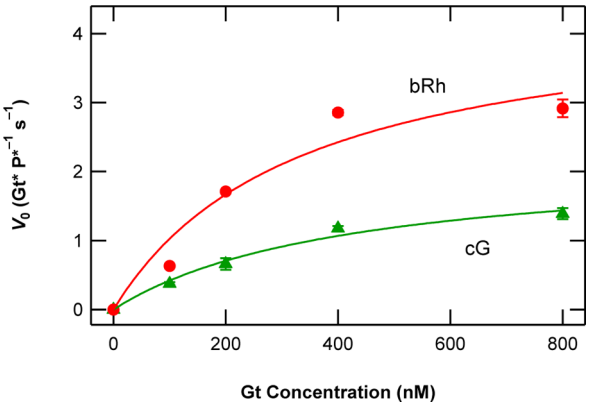

Figure 5. Dependence of the initial velocity of Gt activation on Gt concentration. The initial velocities of Gt activation for bRh (circles) and cG (triangles) per photoactivated pigment (P*) were fit by eq 12. K_M and $V_{\max}$ were estimated to be 333 ± 189 nM and 4.5 ± 1.1 Gt* P*$^{-1}$ s^{-1} for bRh and 420 ± 120 nM and 2.2 ± 0.3 Gt* P*$^{-1}$ s^{-1} for cG, respectively.

The plot was well fit by eq 12, which gave a $V_{\max}$ of 4.5 ± 1.1 Gt* P*$^{-1}$ s^{-1} and a K_M of 333 ± 189 nM for bRh, and a $V_{\max}$ of 2.2 ± 0.3 Gt* P*$^{-1}$ s^{-1} and a K_M of 420 ± 120 nM for cG. The similar K_M but reduced $V_{\max}$ are typical of noncompetitive inhibition. It shows that the binding affinities of photoactivated cG and bRh for Gt are comparable, while the conformational change of Gt induced by bRh results in GDP–GTPγS exchange more efficient than that induced by cG.

The $V_{\max}$ and K_M of bRh estimated here were ~10 times smaller than those reported by Ernst et al. (46 Gt* P*$^{-1}$ s^{-1} and 2.3 μM, respectively),[12] although the velocity was almost saturated at 800 nM Gt (Figure 5). However, at a low concentration of Gt (~1 μM), the velocities are consistent (~3 Gt* P*$^{-1}$ s^{-1}). The disagreement at high Gt concentrations in 0.01% DDM buffer (200 μM DDM) might arise from the difference in the ratio of protein and effective detergent between the preparations.

Because metarhodopsin II is the predominant photoproduct in DDM buffer and the formation of metarhodopsin III is slow (~10 min), metarhodopsin I and metarhodopsin III were not taken into consideration either. However, the photoproduct of cG ~1 s after irradiation is composed of 74% Meta-II and 26% Meta-III (Figure 1). The fluorescence increase for cG was well fit with a single-exponential function in which only decay of Meta-II into opsin and Gt activation by Meta-II are taken into consideration (Figure 4b), although 14% of photoactivated cG remained as Meta-III 20 s after flash irradiation, showing that Gt activation by Meta-III is negligible.

Unlike activation of Gt by bRh, that by cG quickly decelerated because of the ready decay of Meta-II caused by chromophore hydrolysis. On the other hand, the $V_{\max}$ of cG was ~50% of that of bRh. The relationship between these two characteristics of cG was examined using mutants of cG and bRh that have altered lifetimes of their Meta-II states. Glu122 and Ile189 are conserved in the rhodopsin group and are replaced by Gln122 and Pro189, respectively, in cG. It is reported that the E122Q and I189P mutations for rhodopsin facilitate chromophore hydrolysis in Meta-II, while the Q122E and P189I mutations in cG stabilize Meta-II.[8,18] Thus, bRh-E122Q/I189P and cG-Q122E/P189I were subjected to the same kinetic measurements (Figure 4c,d). The absorption maxima and the rate constants of opsin formation estimated from the intrinsic fluorescence increase in the absence of Gt and GTPγS are summarized in Table 1.

Table 1. Characteristics of bRh, cG, and Their Mutants

pigment	$\lambda_{\max}$[a] (nm)	opsin formation[b] (s^{-1})	V_0 (Gt* P*$^{-1}$ s^{-1})
bRh-WT	500	0.00141 ± 0.00001	2.39 ± 0.03
bRh-E122Q/I189P	482	0.0656 ± 0.0014	2.09 ± 0.04
cG-WT	505	0.339 ± 0.011	1.29 ± 0.10
cG-Q122E/P189I	513	0.00893 ± 0.00006	2.29 ± 0.03

[a]Absorption maxima in the dark state. [b]Estimated from the intrinsic fluorescence increase.

A rapid deceleration of Gt activation like that shown by cG was not observed for cG-Q122E/P189I; its opsin formation is suppressed. In contrast, deceleration was observed for bRh-E122Q/I189P; its opsin formation is facilitated. Therefore, these results confirm that the rapid deceleration of cG is mainly ascribed to the fast decay of Meta-II into opsin. Because the fluorescence increase of the pigment was negligible for cG-Q122E/P189I, like that for bRh (Figure 4d, bottom traces), the $V_0^{F(\text{Gt}\rightarrow\text{Gt}^*)}$ for this mutant was estimated solely from the fluorescence increase in the presence of Gt and GTPγS (top traces). In contrast, the fluorescence increase of bRh-E122Q/I189P in the absence of Gt and GTPγS was not negligible on this time scale (Figure 4c). However, the calculation based on eq 11 was not applicable for bRh-E122Q/I189P because opsin formation is not sufficiently fast to neglect the depletion of Gt. It was shown that the rate constant of opsin formation of cG in the presence of Gt and GTPγS was 0.22 s^{-1}, while that in their absence was 0.34 s^{-1} (Figure 4b). Assuming that this ratio is not largely different between cG and bRh-E122Q/I189P, 65%

dx.doi.org/10.1021/bi3015967 | Biochemistry 2013, 52, 3010–3018

of $V_0^{F(MII\rightarrow Ops)}$ measured by bRh-E122Q/I189P alone (bottom trace) was subtracted from $V_0^{F(total)}$ measured in the presence of Gt and GTPγS (top trace). The initial velocity of Gt activation per photoactivated pigment (V_0) was calculated and is shown in Table 1 and Figure 6a (red bars). The number of Gt* molecules 20 s after irradiation is also shown (blue bars) and reveals that the amounts of Gt* for cG and bRh-E122Q/I189P generating short-lived Meta-II were smaller than those expected on the basis of V_0 because of the decay of Meta-II.

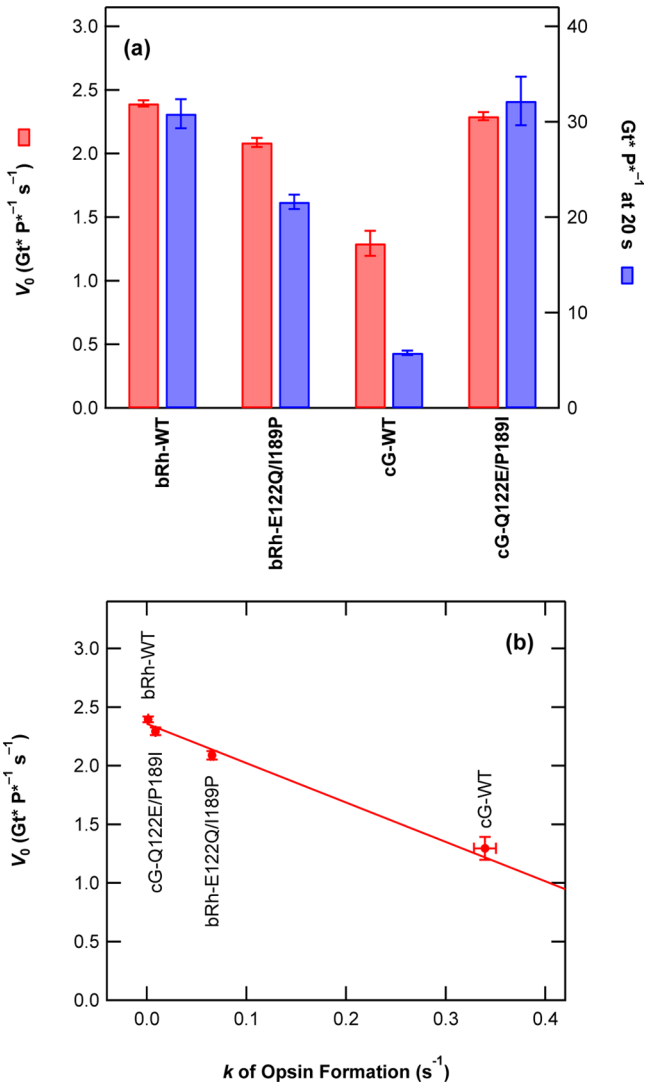

Figure 6. Efficiency of Gt activation by cG, bRh, and their mutants. (a) Initial velocities of Gt activation (red) and the total number of activated Gt molecules 20 s after the flash (blue). (b) Initial velocity of Gt activation plotted vs the rate constant of opsin formation estimated from the intrinsic fluorescence increase of the irradiated pigment.

The V_0 of bRh-E122Q/I189P was significantly smaller than that of bRh. In Figure 6b, the V_0 of cG, bRh, and their mutants was plotted against the rate constant of opsin formation (k_r). They were negatively correlated, suggesting that structures with high Gt activating efficiencies have a retinal Schiff base resistant to hydrolysis and, conversely, structures with low Gt activating efficiencies have a readily hydrolyzable retinal Schiff base.

DISCUSSION

The photon counting system reported here was constructed to detect the intrinsic fluorescence from Trp generated by an excitation beam sufficiently weak so as not to bleach the pigments at a time resolution of 100 ms. Using this system, we demonstrated that the intrinsic fluorescence of Trp is a good probe for detecting the Gt activation by the cone pigment, as it is for rhodopsin.[12] In addition, the release of all-*trans*-retinal from the bleached cone pigment is also detected using this system. Our kinetic analysis characterized the process of activation of Gt by the cone pigment.

Light-Induced Structural Changes of Rod and Cone Visual Pigments. GPCR activates its cognate G protein via rearrangement of the transmembrane helices in response to stimuli.[27] This kinetic analysis demonstrated that the V_{max} of Gt activation by photoactivated cG was ~50% of that of bRh, but the K_M of Gt activation by cG and bRh was comparable (Figure 5). On the other hand, Gt activation by cG was quickly decelerated because of the decay of Meta-II, as shown by the characterizations of the bRh mutant generating short-lived Meta-II (bRh-E122Q/I189P) and the cG mutant generating long-lived Meta-II (cG-Q122E/P189I) (Figure 4). In addition, the V_0 of Gt activation was negatively correlated with the rate constant of opsin formation (k_r) (Figure 6b).

Opsin is formed by the hydrolysis of the retinal Schiff base. It has been reported that the water molecule for the hydrolysis of the Schiff base is provided from the bulk water.[28] Therefore, these results indicate that the retinal Schiff base of photoactivated cG is significantly more solvent-accessible than that of bRh. However, the hydrolysis of Meta-II is suppressed by forming a complex with HAP or Gt (Figure 2). Therefore, Gt binding induces a conformational change of the structure of Meta-II of cG into one similar to that of metarhodopsin II, in which the path of the water molecule is closed. This is consistent with the finding that the stabilizing effect of HAP on the hydrolysis of metarhodopsin II is very small.[29] The negative correlation between k_r and V_0 for cG, bRh, and their mutants suggests that a pigment whose Meta-II readily adopts a metarhodopsin-II-like structure in the absence of Gt has a high Gt activation efficiency.

Rhodopsin has evolved from a cone visual pigment to be specialized for twilight vision.[30] The amino acid sequence of bRh (348 amino acid residues) has 98 substitutions and seven deletions as compared to that of cG (355 amino acid residues) (Figure S2 of the Supporting Information). Among them, two substitutions (at positions 122 and 189) cause switching between the activation efficiencies of cG and bRh.

It has been reported that Glu122 in metarhodopsin II is hydrogen-bonded with His211, which stabilizes the active conformation.[31] Loss of this hydrogen bond would reduce the activation efficiency. A Ramachandran diagram shows that the dihedral angles of Ile189 in both dark state bRh [Protein Data Bank (PDB) entry 1U19] and active state (PDB entries 3PQR and 2X72) are positioned in the allowed region of proline. Thus, it is unlikely that the mutation from Ile to Pro results in a substantial difference in the backbone structure. The side chain of Ile189 is proximate to C19 (9-methyl group) of the chromophore, which affects the efficiency of Gt activation.[32,33] However, because the replacements of these residues could not fully restore the characteristics of the parent pigments, other residues must further contribute to the differences between cG and bRh.

dx.doi.org/10.1021/bi3015967 | *Biochemistry* 2013, 52, 3010−3018

The invertebrate rhodopsin is photoconverted to the Meta intermediate, whose chromophore is resistant to the hydrolysis, but the Gt activation efficiency is substantially lower ($^1/_{10}$ to $^1/_{50}$) than that of bRh. Our finding that the Gt activation efficiency of photoactivated cG was approximately half that of bRh indicates that cG adopts an open structure like the Gt-activating state of vertebrate rhodopsin. As a result, bulk water molecules became more accessible to the retinal Schiff base. Rhodopsin has further evolved from a cone pigment to generate a stable Gt-activating state by suppressing the conformational fluctuation.

Interaction between cG and Rod-Type Gt. In this study, to strictly compare the Gt activation efficiency of the cone pigment with that of rhodopsin, bovine rod Gt was used for both pigments. The crystal structure of the complex composed of metarhodopsin II and HAP has shown that Leu72, Arg135, Val138, Val139, Lys141, Ala233, Thr242, Thr243, Ala246, Glu249, Val250, Met253, Met257, Asn310, and Gln312 of metarhodopsin II are within ∼4 Å of the HAP (Figure S3 of the Supporting Information).[34,35] These residues are perfectly conserved among cG, cRh, and bRh. On the other hand, the second and third cytoplasmic loops of metarhodopsin II are involved in the interaction with Gt. As shown in the Supporting Information, the amino acid sequences of these regions are highly conserved. Therefore, with respect to the amino acid sequence, it is likely that the interface between cG and cone Gt is essentially identical to that between rhodopsin and rod Gt. In fact, it has been demonstrated that rod and cone Gt α-subunits in mice are functionally interchangeable.[36,37] Thus, it is unlikely that an artifact arose from the mismatch between cG and bovine rod Gt.

Physiological Relevance of the Lifetime of Meta-II. The lifetime of metarhodopsin II appears to be much longer than expected from its role in the Gt activation process in the cell. Meta-II is deactivated by phosphorylation by a kinase.[6,38,39] The turnover of the phosphorylation of mouse rhodopsin at 37 °C is estimated to be 1−3 s^{-1}.[40] Because this is significantly faster than the decay of metarhodopsin II (∼150 s),[29] the thermal decay of metarhodopsin II is not responsible for the shutdown of rods. In fact, while the Gt activation efficiency of Meta-II of cG *in vitro* is 70 times lower than that of metarhodopsin II (Figure 3), the difference is very small in the cell (1−3 times), as shown by the electrophysiology of rods in which cone pigments are expressed.[41,42] On the other hand, the decay time constant of Meta-II of cG was estimated to be 2.9 s at 20 °C and was increased to 60 s at 2 °C. Thus, the decay time constant of Meta-II at 37 °C is roughly estimated to be 200 ms. Our results show that the activation of Gt by cG is spontaneously quenched by the decay of Meta-II. Assuming that the visual transduction cascade in the cell is shut down in 100 ms and Meta-II decays in a first-order reaction with a time constant of 200 ms, 40% of Meta-II decays before the shutdown. Thus, for the cone pigment, spontaneous deactivation by the stochastic decay of Meta-II takes place prior to the deactivation induced by the regulation system in the cell. Under very dim light conditions in which a visual cell is activated by a single photon, the stochastic decay of a single molecule of Meta-II causes quenching of the signal transduction in the cell. Because the thermal decay of a single Meta-II molecule occurs randomly, such decay before sufficient amplification of the signal causes fluctuation of the cell response to a single photon. However, if the lifetime of Meta-II is prolonged by 100-fold, as it is for rhodopsin, only 0.5% of Meta-II decays within 100 ms. The lifetime of metarhodopsin II seems to be unnecessarily long for achieving Gt activation efficiency in rods, but it would be essential for detecting a single photon.

■ ASSOCIATED CONTENT

Supporting Information

SVD analysis of the transient UV−visible absorption spectra of cG (Figure S1), crystal structure of the cytoplasmic surface of metarhodopsin II (Figure S2), and interaction of metarhodopsin II and the C-terminal peptide derived from the Gt α-subunit (Figure S3). This material is available free of charge via the Internet at http://pubs.acs.org.

■ AUTHOR INFORMATION

Corresponding Author

*Department of Biophysics, Graduate School of Science, Kyoto University, Kyoto 606-8502, Japan. Telephone: +81-75-753-4213. Fax: +81-75-753-4210. E-mail: shichida@rh.biophys.kyoto-u.ac.jp.

Funding

This work was supported by the Japanese Ministry of Education, Culture, Sports, Science, and Technology [Grants-in-aid for Scientific Research to Y.I. (23370070), T.Y. (23770074), and Y.S. (20227002) and Grants for Excellent Graduate Schools] and by a grant from the Takeda Science Foundation to T.Y.

Notes

The authors declare no competing financial interest.

■ ACKNOWLEDGMENTS

We are grateful to Dr. Elizabeth Nakajima for critical reading of our manuscript and invaluable comments.

■ ABBREVIATIONS

Gt, transducin; cG, chicken green-sensitive cone visual pigment; bRh, bovine rhodopsin; WT, wild type; HEPES, 2-[4-(2-hydroxyethyl)-1-piperazinyl]ethanesulfonic acid; DDM, *n*-dodecyl β-D-maltoside; HAP, high-affinity peptide; CHAPS, 3-[(3-cholamidopropyl)dimethylammonio]propanesulfonate; PC, L-α-phosphatidylcholine; Meta-I, Meta-II, and Meta-III, bleaching intermediates of the cone visual pigment corresponding to metarhodopsin I, metarhodopsin II, and metarhodopsin III, respectively.

■ REFERENCES

(1) Shichida, Y., and Matsuyama, T. (2009) Evolution of opsins and phototransduction. *Philos. Trans. R. Soc., B 364*, 2881−2895.

(2) Shichida, Y., Imai, H., Imamoto, Y., Fukada, Y., and Yoshizawa, T. (1994) Is chicken green-sensitive cone visual pigment a rhodopsin-like pigment? A comparative study of the molecular properties between chicken green and rhodopsin. *Biochemistry 33*, 9040−9044.

(3) Okada, T., Matsuda, T., Kandori, H., Fukada, Y., Yoshizawa, T., and Shichida, Y. (1994) Circular dichroism of metaiodopsin II and its binding to transducin: A comparative study between meta II intermediates of iodopsin and rhodopsin. *Biochemistry 33*, 4940−4946.

(4) Imai, H., Imamoto, Y., Yoshizawa, T., and Shichida, Y. (1995) Difference in molecular properties between chicken green and rhodopsin as related to the functional difference between cone and rod photoreceptor cells. *Biochemistry 34*, 10525−10531.

(5) Imai, H., Terakita, A., Tachibanaki, S., Imamoto, Y., Yoshizawa, T., and Shichida, Y. (1997) Photochemical and biochemical properties

of chicken blue-sensitive cone visual pigment. *Biochemistry 36*, 12773−12779.
(6) Tachibanaki, S., Tsushima, S., and Kawamura, S. (2001) Low amplification and fast visual pigment phosphorylation as mechanisms characterizing cone photoresponses. *Proc. Natl. Acad. Sci. U.S.A. 98*, 14044−14049.
(7) Okano, T., Fukada, Y., Shichida, Y., and Yoshizawa, T. (1992) Photosensitivities of iodopsin and rhodopsins. *Photochem. Photobiol. 56*, 995−1001.
(8) Kuwayama, S., Imai, H., Hirano, T., Terakita, A., and Shichida, Y. (2002) Conserved proline residue at position 189 in cone visual pigments as a determinant of molecular properties different from rhodopsins. *Biochemistry 41*, 15245−15252.
(9) Imai, H., Kojima, D., Oura, T., Tachibanaki, S., Terakita, A., and Shichida, Y. (1997) Single amino acid residue as a functional determinant of rod and cone visual pigments. *Proc. Natl. Acad. Sci. U.S.A. 94*, 2322−2326.
(10) Phillips, W. J., and Cerione, R. A. (1988) The intrinsic fluorescence of the α subunit of transducin. Measurement of receptor-dependent guanine nucleotide exchange. *J. Biol. Chem. 263*, 15498−15505.
(11) Faurobert, E., Otto-Bruc, A., Chardin, P., and Chabre, M. (1993) Tryptophan W207 in transducin Tα is the fluorescence sensor of the G protein activation switch and is involved in the effector binding. *EMBO J. 12*, 4191−4198.
(12) Ernst, O. P., Gramse, V., Kolbe, M., Hofmann, K. P., and Heck, M. (2007) Monomeric G protein-coupled receptor rhodopsin in solution activates its G protein transducin at the diffusion limit. *Proc. Natl. Acad. Sci. U.S.A. 104*, 10859−10864.
(13) Farrens, D. L., and Khorana, H. G. (1995) Structure and function in rhodopsin. Measurement of the rate of metarhodopsin II decay by fluorescence spectroscopy. *J. Biol. Chem. 270*, 5073−5076.
(14) Hoersch, D., Otto, H., Wallat, I., and Heyn, M. P. (2008) Monitoring the conformational changes of photoactivated rhodopsin from microseconds to seconds by transient fluorescence spectroscopy. *Biochemistry 47*, 11518−11527.
(15) Chen, M. H., Kuemmel, C., Birge, R. R., and Knox, B. E. (2012) Rapid release of retinal from a cone visual pigment following photoactivation. *Biochemistry 51*, 4117−4125.
(16) Nathans, J. (1990) Determinants of visual pigment absorbance: Role of charged amino acids in the putative transmembrane segments. *Biochemistry 29*, 937−942.
(17) Imai, H., Terakita, A., and Shichida, Y. (2000) Analysis of amino acid residues in rhodopsin and cone visual pigments that determine their molecular properties. *Methods Enzymol. 315*, 293−312.
(18) Kuwayama, S., Imai, H., Morizumi, T., and Shichida, Y. (2005) Amino acid residues responsible for the meta-III decay rates in rod and cone visual pigments. *Biochemistry 44*, 2208−2215.
(19) Tachibanaki, S., Imai, H., Mizukami, T., Okada, T., Imamoto, Y., Matsuda, T., Fukada, Y., Terakita, A., and Shichida, Y. (1997) Presence of two rhodopsin intermediates responsible for transducin activation. *Biochemistry 36*, 14173−14180.
(20) Martin, E. L., Rens-Domiano, S., Schatz, P. J., and Hamm, H. E. (1996) Potent peptide analogues of a G protein receptor-binding region obtained with a combinatorial library. *J. Biol. Chem. 271*, 361−366.
(21) Sakai, K., Imamoto, Y., Su, C. Y., Tsukamoto, H., Yamashita, T., Terakita, A., Yau, K. W., and Shichida, Y. (2012) Photochemical nature of parietopsin. *Biochemistry 51*, 1933−1941.
(22) Imamoto, Y., and Shichida, Y. (2008) Thermal recovery of iodopsin from photobleaching intermediates. *Photochem. Photobiol. 84*, 941−948.
(23) Sato, K., Yamashita, T., Imamoto, Y., and Shichida, Y. (2012) Comparative studies on the late bleaching processes of four kinds of cone visual pigments and rod visual pigment. *Biochemistry 51*, 4300−4308.
(24) König, B., Welte, W., and Hofmann, K. P. (1989) Photo-activation of rhodopsin and interaction with transducin in detergent micelles. Effect of 'doping' with steroid molecules. *FEBS Lett. 257*, 163−166.
(25) Imamoto, Y., Kataoka, M., Tokunaga, F., and Palczewski, K. (2000) Light-induced conformational changes of rhodopsin probed by fluorescent Alexa594 immobilized on the cytoplasmic surface. *Biochemistry 39*, 15225−15233.
(26) Sato, K., Morizumi, T., Yamashita, T., and Shichida, Y. (2010) Direct observation of the pH-dependent equilibrium between metarhodopsins I and II and the pH-independent interaction of metarhodopsin II with transducin C-terminal peptide. *Biochemistry 49*, 736−741.
(27) Deupi, X., and Standfuss, J. (2011) Structural insights into agonist-induced activation of G-protein-coupled receptors. *Curr. Opin. Struct. Biol. 21*, 541−551.
(28) Jastrzebska, B., Palczewski, K., and Golczak, M. (2011) Role of bulk water in hydrolysis of the rhodopsin chromophore. *J. Biol. Chem. 286*, 18930−18937.
(29) Heck, M., Schadel, S. A., Maretzki, D., Bartl, F. J., Ritter, E., Palczewski, K., and Hofmann, K. P. (2003) Signaling states of rhodopsin. Formation of the storage form, metarhodopsin III, from active metarhodopsin II. *J. Biol. Chem. 278*, 3162−3169.
(30) Okano, T., Kojima, D., Fukada, Y., Shichida, Y., and Yoshizawa, T. (1992) Primary structures of chicken cone visual pigments: Vertebrate rhodopsins have evolved out of cone visual pigments. *Proc. Natl. Acad. Sci. U.S.A. 89*, 5932−5936.
(31) Weitz, C. J., and Nathans, J. (1992) Histidine residues regulate the transition of photoexcited rhodopsin to its active conformation, metarhodopsin II. *Neuron 8*, 465−472.
(32) Das, J., Crouch, R. K., Ma, J. X., Oprian, D. D., and Kono, M. (2004) Role of the 9-methyl group of retinal in cone visual pigments. *Biochemistry 43*, 5532−5538.
(33) Estevez, M. E., Kolesnikov, A. V., Ala-Laurila, P., Crouch, R. K., Govardovskii, V. I., and Cornwall, M. C. (2009) The 9-methyl group of retinal is essential for rapid Meta II decay and phototransduction quenching in red cones. *J. Gen. Physiol. 134*, 137−150.
(34) Choe, H. W., Kim, Y. J., Park, J. H., Morizumi, T., Pai, E. F., Krauss, N., Hofmann, K. P., Scheerer, P., and Ernst, O. P. (2011) Crystal structure of metarhodopsin II. *Nature 471*, 651−655.
(35) Standfuss, J., Edwards, P. C., D'Antona, A., Fransen, M., Xie, G., Oprian, D. D., and Schertler, G. F. (2011) The structural basis of agonist-induced activation in constitutively active rhodopsin. *Nature 471*, 656−660.
(36) Deng, W. T., Sakurai, K., Liu, J., Dinculescu, A., Li, J., Pang, J., Min, S. H., Chiodo, V. A., Boye, S. L., Chang, B., Kefalov, V. J., and Hauswirth, W. W. (2009) Functional interchangeability of rod and cone transducin α-subunit. *Proc. Natl. Acad. Sci. U.S.A. 106*, 17681−17686.
(37) Gopalakrishna, K. N., Boyd, K. K., and Artemyev, N. O. (2012) Comparative analysis of cone and rod transducins using chimeric Gα subunit. *Biochemistry 51*, 1617−1624.
(38) Bownds, D., Dawes, J., Miller, J., and Stahlman, M. (1972) Phosphorylation of frog photoreceptor membranes induced by light. *Nat. New Biol. 237*, 125−127.
(39) Kühn, H., Cook, J. H., and Dreyer, W. J. (1973) Phosphorylation of rhodopsin in bovine photoreceptor membranes. A dark reaction after illumination. *Biochemistry 12*, 2495−2502.
(40) Kennedy, M. J., Lee, K. A., Niemi, G. A., Craven, K. B., Garwin, G. G., Saari, J. C., and Hurley, J. B. (2001) Multiple phosphorylation of rhodopsin and the in vivo chemistry underlying rod photoreceptor dark adaptation. *Neuron 31*, 87−101.
(41) Sakurai, K., Onishi, A., Imai, H., Chisaka, O., Ueda, Y., Usukura, J., Nakatani, K., and Shichida, Y. (2007) Physiological properties of rod photoreceptor cells in green-sensitive cone pigment knock-in mice. *J. Gen. Physiol. 130*, 21−40.
(42) Shi, G., Yau, K. W., Chen, J., and Kefalov, V. J. (2007) Signaling properties of a short-wave cone visual pigment and its role in phototransduction. *J. Neurosci. 27*, 10084−10093.